IUST Iran University of Science and Technology

Iranian Journal of Electrical and Electronic Engineering

Journal Homepage: ijeee.iust.ac.ir

Research Paper

An Improved Motion Vector Estimation Approach for Video Error Concealment Based on the Video Scene Analysis

S. M. Zabihi*, H. Ghanei-Yakhdan*(C.A.), and N. Mehrshad**

Abstract: In order to enhance the accuracy of the motion vector (MV) estimation and also reduce the error propagation issue during the estimation, in this paper, a new adaptive error concealment (EC) approach is proposed based on the information extracted from the video scene. In this regard, the motion information of the video scene around the degraded MB is first analyzed to estimate the motion type of the degraded MB. If the neighboring MBs possess uniform motion, the degraded MB imitates the behavior of neighboring MBs by choosing the MV of the collocated MB. Otherwise, the lost MV is estimated through the second proposed EC technique (i.e., IOBMA). In the IOBMA, unlike the conventional boundary matching criterion-based EC techniques, not only each boundary distortion is evaluated regarding both the luminance and the chrominance components of the boundary pixels, but also the total boundary distortion corresponding to each candidate MV is calculated as the weighted average of the available boundary distortions. Compared with the state-of-the-art EC techniques, the simulation results indicate the superiority of the proposed EC approach in terms of both the objective and subjective quality assessments.

Keywords: Temporal Error Concealment, Video Scene, Weighted Averaging, Motion Vector Estimation, H.264/AVC.

1 Introduction

GREAT advances in communications technology in recent years have inspired the use of various and attractive communication services, such as multimedia services, through wireless channels. However, the growing demand for multimedia services, and particularly the video services, imposes additional burdens on the different parts of the transmission schemes, especially on the source coding techniques and the error control techniques.

Despite the great advances in improving the spectral efficiency of the modern communication systems, such as the OFDM modulation technique, due to the huge amount of the raw video sequences data, the bandwidth scarcity issue is still the major challenge in video services. Therefore, since the 1990s, ISO/IEC and ITU-T have proposed some block-based video coding standards, such as MPEG-4, H.264/AVC, and the latest H.265/HEVC, to compress the raw video data by eliminating the existing redundancies within the video sequences.

Although the problem of the high amount of the video data is to a great extent addressed through the proposed video compression standards, high compression efficiency increases the vulnerability of the video stream to the transmission errors. Moreover, as the predictive and variable length coding are exploited in the encoder to compress the video data, transmission errors not only degrade the quality of the current frame but also propagates to the subsequent frames.

Regardless of the type of the transmitted data, some error control approaches are proposed to increase the robustness of the transmitted data against the channel errors, such as the Forward Error Correction (FEC) and Automatic Repeat Request (ARQ) [1]. However, in these methods, the robustness is achieved at the expense of reduced bandwidth efficiency. Moreover, these

Iranian Journal of Electrical and Electronic Engineering, 2020.
Paper first received 06 November 2019, revised 23 March 2020, and accepted 28 May 2020.
* The authors are with the Electrical Engineering Department, Yazd University, Yazd, Iran.
E-mails: mzabihi@stu.yazd.ac.ir and hghaneiy@yazd.ac.ir.
** The author is with the Electrical and Computer Engineering Department, University of Birjand, Birjand, Iran.
E-mail: nmehrshad@birjand.ac.ir.
Corresponding Author: H. Ghanei-Yakhdan.

methods are known to work well only for low error rates and their performances tend to degrade in high error rates.

As illustrated in Fig. 1, in addition to the aforementioned techniques, there are two other categories of error control techniques designed specifically for the video data: Error resilience and error concealment methods.

Error resilience methods such as the Multiple Description Coding (MDC), are applied at the encoder and exploit the redundancies due to high spatial and/or temporal correlation within the video sequence to make the encoded video more robust against the transmission errors [2-8]. However, similar to the conventional error control methods, the robustness is achieved at the expense of reduced bandwidth efficiency. Moreover, these methods cannot thoroughly prevent the received video sequences degraded due to the transmission error.

Unlike the error resilience methods, the error concealment (EC) techniques are applied at the receiver side and take the redundancies within the video sequence to reconstruct the erroneous regions of the frames. Therefore, there is no or small need to modify the encoder or channel coding schemes [9], leading to better bandwidth efficiency.

According to the type of redundancies exploited for reconstructing the damaged regions, existing EC techniques can be classified into two general categories: Spatial Error Concealment (SEC) techniques, Temporal Error Concealment (TEC) techniques.

SEC techniques employ the local correlation of the correct neighboring regions within the degraded frame to reconstruct the lost regions. However, in addition to the high computational complexity due to the pixel-wise interpolation, the performance of the SEC techniques is highly dependent on the neighboring correct MacroBlocks (MBs), so that their performance tends to degrade in the presence of the slice error, where the number of correct neighboring MBs decreases. In addition, the SEC techniques suffer the blurring effect which reduces their capability in reconstructing the structures (i.e., the objects or regions within the frame which can be separated by a border).

TEC techniques, however, exploit the strong inter-frame correlation to find the most appropriate portion of the reference frame and replace it with the lost MB in the current frame. Unlike the SEC techniques, since the structures within the MB are maintained during the replacement, the TEC techniques are more capable of reconstructing the structures and hence, provide better reconstruction quality than the SEC techniques, especially in the presence of slice error. However, the performance of the TEC techniques greatly depends on the correct estimation of the lost Motion Vector (MV), so that the inaccurate estimation of the lost MVs, even as much as a few pixels, can lead to blocky artifact issue which is not pleasant to the viewers. Besides, in video sequences with the IPPP picture structure in which each frame serves as the reference frame for its consecutive frame, the distortions due to the inaccurate MVs estimation are not limited to the erroneous frame and propagate to the subsequent frames. This is also the case for reconstructing the other degraded MBs of the erroneous frame so that the previously inaccurately estimated MVs introduce an adverse effect to the results of the MV estimation for the remaining degraded MVs in the frame.

Therefore, to reduce the effect of the error propagation issue on the estimation of the degraded MVs and increase the accuracy of the estimated MVs, in this paper, a new EC approach is proposed exploiting two new EC techniques in an adaptive manner. The first EC technique which is the modified version of the boundary matching algorithm improves the performance of the EC in two ways: first, unlike the traditional boundary matching criterion-based TEC techniques in which the

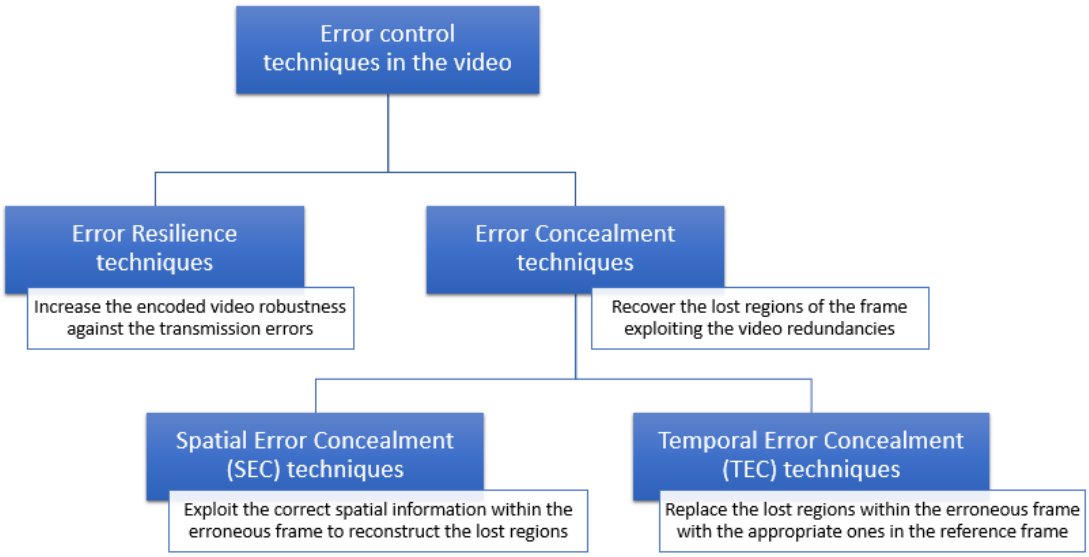

Fig. 1 Classification of the error control techniques in the video sequences.

boundary matching is measured as the difference between the brightness values of the degraded MB and its neighboring MBs, the color information of the MBs are also used to provide a more accurate estimate of the degraded MV. Second, to make the proposed EC technique more robust against the error propagation issue, the total boundary distortion corresponding to each candidate MV is calculated as the weighted average of the boundary distortions between the degraded MB and the candidate MB. However, unlike the conventional boundary matching criterion-based TEC techniques, the previously reconstructed MBs are discriminated from the intact MBs through the different weights assigned to them.

In addition, since the boundary matching criterion-based TEC techniques exploit the spatial information within the frames to estimate the MVs of the degraded MBs, the performance of the EC techniques is exposed to severe degradation in situation where the reliability of the spatial information in the frame decreases, such as in the presence of slice error with high Block Loss Rate (BLR). Hence, to avoid the performance of the EC technique degraded a lot under such conditions, other information, such as the motion type of the objects in the video sequence, is also extracted from the video scene. For this purpose, before applying the IOBMA, the MVs of the MBs neighboring to the degraded MB (including the correct and the previously reconstructed MBs) are investigated for the uniform motion type. If the neighboring MBs possess the uniform movements in the consecutive frames, the degraded MB tries to imitate the behavior of the neighboring MBs by selecting the collocated MV in the previous frame. Otherwise, the IOBMA is exploited to recover the lost MV.

The main contributions of the paper are summarized as follows:

- Exploiting both the color and reliability of the spatial information of the neighboring MBs to improve the performance of the boundary matching algorithm such as the OBMA.
- Exploiting the motion information of the objects extracted from the video scene to avoid the poor performance of the EC technique in conditions where the reliability of the spatial information in the frame decreases, such as the presence of slice error with high Block Loss Rate in the frame.

The rest of the paper is organized as follows. Section 2 provides a brief overview of the EC techniques proposed in the video EC domain. The proposed EC approach is described in detail in Section 3. The experimental framework and the results of the performance evaluations are presented in Section 4. Finally, the proposed approach is concluded in Section 5.

2 Related Work

As mentioned in the previous section, the EC techniques can be classified into two major categories of the spatial and the temporal EC techniques. In the following a brief introduction to some works carried out in the video EC domain is presented.

2.1 SEC Techniques

As mentioned before, the SEC techniques usually exploit the spatial information within the frame and reconstruct the lost regions through the pixel-wise interpolation/extrapolation. In this regard, Li *et al.* [10] proposed a 4-step adaptive EC process which decides on the appropriate EC technique based on the texture complexity of the neighboring MBs. To reduce the error propagation issue, they proposed the separately-directional interpolation in which the corrupted MB is first divided into finer sub-blocks and then, each finer sub-block is adaptively reconstructed through one of the Bilinear Interpolation and Directional Interpolation techniques. H. Ni and Y. Li [11] proposed adaptive edge thresholding and directional weight to estimate the significant edges of missing MBs and solve the problem of conventional directional interpolation methods. Liu *et al.* [9] exploit a pixel-wise adaptive predictor to estimate the missing pixels of the lost regions sequentially. To tune the support shape and the order of the predictor, a model selection problem is defined and solved with the Bayesian Information Criterion (BIC). Besides, to handle the error propagation issue, the pixels are selected for EC in order of the self-designed uncertainty. Akbari *et al.* [12] proposed a sparse spatial error concealment technique in which, the sparse representation of the corrupted patch is first computed through the corrupted dataset dictionary and then, the corrupted patch is reconstructed through the original dataset dictionary. To reduce the blurring issue of the SEC techniques and persevere the image sharpness and the continuity of edges in the erroneous region of the I-frame, Mohammadzadeh Qaratlu *et al.* [13] proposed a directional extrapolation which tries to extrapolate each missing pixel along its specific direction calculated previously in the EC process. Adaptive exploitation of the exemplar-based image inpainting and the spatial interpolation are presented in [14]. In the proposed technique, the exemplar-based technique is applied to the regions with regular structures, whereas in the complex regions with irregular structures, EC is performed through either the directional interpolation or neighbor interpolation, based on the gradient information. Comparison between two categories of the SEC techniques, namely the Frequency Selective Extrapolation and the exemplar-based EC algorithms, yields the superiority of the Frequency Selective Extrapolation method over the patch matching algorithm in the presence of distinct random block loss [15]. As mentioned in Section 1, the EC techniques usually try to reconstruct the degraded region within the frame with no modification to the encoder. Recently,

however, an encoder-based error concealment method is proposed for the image inpainting purpose which models the error concealment problem as a sparse recovery framework [16]. To this end, in the encoder, the coefficients resulting from applying the wavelet decomposition to the input image are first partitioned into non-overlapping spatial trees (STs). Then, each ST is further projected onto a random basis to provide the sparse recovery framework. At the receiver, given the fact that the wavelet decomposition has a tree-sparse structure, an iterative sparse reconstruction algorithm is applied to the erroneous image to recover the lost regions. Simulation results indicate that the proposed encoder-based EC technique outperforms the state-of-the-art image inpainting techniques.

2.2 TEC Techniques

Contrary to the SEC, the TEC techniques take the temporal redundancies to estimate the MVs of the lost MBs. The Boundary Matching Algorithm (BMA) [17] is one of the most famous and well-known TEC techniques in this category. In the BMA, the MV of the degraded MB is picked out from a set of the candidate MVs according to a boundary matching criterion (BMC) defined between the inner boundaries of the candidate MB and the outer boundaries of the degraded MB. To improve the performance of the BMA, Thaipanich *et al.* [18] proposed to apply the BMC between the outer boundaries of both the candidate MB and the degraded MB. Unlike the conventional TEC techniques, in which the appropriate MB for motion compensation is selected only from the previous frame (i.e., the reference frame), Yu *et al.* [19] proposed a multiple-reference EC algorithm which explores 5 previous frames for the most appropriate MB in half- and quarter-pixel motion estimation. In addition to the information of the MVs in the video scene, Lin *et al.* exploited the other information, such as the residual information and partition information, as the reliability measure to enhance the accuracy of the MV estimation [20, 21]. In contrast to traditional boundary matching algorithms which utilize one BMC to recover the degraded MVs, Chen *et al.* [22] proposed an EC algorithm which exploits two BMCs, including an external boundary matching (EBM) and a directional boundary matching (DBM) criteria, adaptively. The proposed method in [23] further improves the performance of the DBM algorithm. Marvasti-Zadeh *et al.* [24] also proposed an EC algorithm which exploits two BMCs, including outer boundary matching (OBM) and a directional temporal boundary matching (DTBM) criteria, adaptively. Simulation results yield the superiority of the proposed EC algorithm over both the OBMA and DTBMA techniques. Lie *et al.* [25] proposed an iterative Dynamic Programming (DP)-based approach which utilizes DP optimization technique to estimate the lost MVs in a global manner. Wei *et al.* [26] proposed a propagation-based MV estimation which splits each degraded MB to finer sub-blocks and then, estimates the MV of each sub-block as the average MV of the available neighboring sub-blocks. In heavily corrupted videos the number of the correct MBs neighboring to the degraded MB decreases, thereby reducing the accuracy of the MVs estimation. From this viewpoint, the estimated MVs can be regarded as the noisy MVs and thus, the noise reduction techniques can be exploited to increase the accuracy of the estimated MV. Accordingly, the noise reduction capability of the Kalman and particle filters is exploited in [27-29]. In [30], however, the neural networks are exploited to track the variations of the MVs in the consecutive frames and reduce the estimation noise. Chen *et al.* [31] proposed a two-stage EC approach including a spatio-temporal boundary matching algorithm to estimate an MV for the degraded MB and a partial differential equation (PDE) based algorithm. In the first stage, the MV of the degraded MB is estimated exploiting both the temporal and spatial smoothness properties of the video sequences in a weighted manner. In this regard, the average changes of the Laplacian estimator along the tangent direction is exploited as the spatial boundary criterion. Regarding the temporal smoothness property, however, similar to the conventional OBMA [18], the average difference between the external boundaries of the reference MB and the lost MBs is selected as the temporal boundary criterion. In the second stage, unlike the traditional TEC techniques in which the degraded MB is replaced directly with the reference MB corresponding to the estimated MV, the degraded MB is reconstructed so that, under given boundary condition, its gradient field has the least difference with the gradient field of the reference MB. The proposed method can reduce the blocking artifact and well-preserve the inner structure of the reconstructed MBs.

3 Proposed EC Approach

In order to focus on the design of the proposed EC approach, in this paper it is supposed that the positions of the degraded MBs in the frame are known. There are several papers concerning the error detection in the video sequences [32-36] which can be used for this purpose. Then, according to the position of the erroneous MBs in the frame two error models can be considered: *Random error* and *Slice error*. As illustrated in Fig. 2, the *Slice error* (right Figure) appears as a whole row loss, whereas in the *Random error* (left Figure) the erroneous MBs are distributed randomly in the frame.

In the following, to outline the proposed EC approach, the video sequence is regarded as $\boldsymbol{f}(x,y,t)$ whose spatial and temporal coordinates are denoted by (x,y) and t, respectively. By definition, $\boldsymbol{f}(x,y,t=\tau)$ is a 3-elements vector containing the luminance and the chrominance

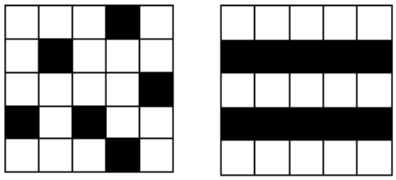

Fig. 2 Illustration of typical block loss. Each square represents an MB with a fixed size of 16 by 16 pixels. The black squares are the lost MBs while the white squares denote the correctly received MBs.

components of the pixel located at position (x,y) in the frame $t = \tau$. These components are represented also by $f_y(x,y,t)$, $f_u(x,y,t)$, and $f_v(x,y,t)$, respectively. Accordingly, an error occurred during the decoding or transmission results in a lost MB whose top-left corner is located at position $p = (x,y)$.

As mentioned previously, the distortions due to the inappropriate reconstruction of the lost regions not only propagate to the subsequent frames but also may reduce the accuracy of the MV estimation for the remaining degraded MBs in the frame. Therefore, in this paper, a new adaptive EC approach is proposed to enhance the performance of the boundary matching criterion-based TEC techniques and provide better reconstruction quality, especially in high BLRs.

As illustrated in Fig. 3 the proposed EC approach first tries to estimate the motion type of the degraded MB from the complexity or uniformity point of view. In this regard, the MVs of the MBs neighboring to the degraded MB are first analyzed for the existence of the uniform motion type. If the neighboring MBs belonging to an object possess the uniform motion type, since the MBs within an object often represent the same MVs in a video sequence, the MV of the degraded MB is also likely to be uniform.

Hence, to verify whether the neighboring MBs follow the uniform motion or not, the dispersion of the neighboring MVs and the corresponding collocated MVs need to be calculated. However, since the position of the degraded MB in the object is random, as illustrated in Fig. 4, five models of the neighborhood are defined for each lost MB. Then, the dispersion of the amplitudes of the differences between the neighboring MVs and the corresponding collocated MVs are calculated using (1)-(3) and the model with the minimum dispersion is selected as the optimum MV set. Finally, if the dispersion in the optimum MV set is less than the predefined threshold in Fig. 5, the degraded MB is classified as the uniform motion MB and hence, the MV of the collocated MB in the reference frame is selected as the MV of the degraded MB. In this paper, the threshold value is set to 1×10^{-5}.

In (1)-(4), $MV\_Set_i^k$ represents the set of the available neighboring MVs of the i-th MB corresponding to the model (k). $Mg\_Set_i^k$ represents the amplitudes of the temporal differences between the MVs of the k-th neighborhood model and their corresponding collocated

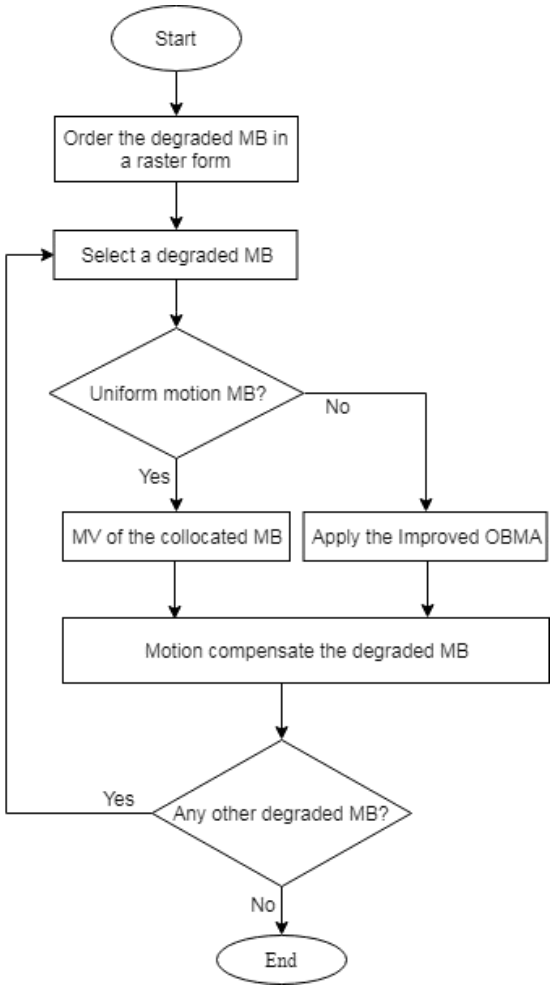

Fig. 3 Schematic diagram of the proposed EC approach.

$$MV\_Set_i^k = \bigcup_{\substack{j \neq i \\ j \in model(k)}} MV_j^{(t)} \qquad 1 \le k \le 5 \tag{1}$$

$$Mg\_Set_i^k = \bigcup_{\substack{j \neq i \\ j \in model(k)}} \left| MV_j^{(t)} - MV_j^{(t-1)} \right| \quad 1 \le k \le 5 \tag{2}$$

$$k_{opt\_Amp} = \arg\min_{k=1,\ldots,5} \left\| Mg\_Set_i^k \right\|_2 \tag{3}$$

$$Mg_i^{opt} = \left\| Mg\_Set_i^{k_{opt\_Amp}} \right\|_2 \tag{4}$$

MVs in the reference frame, respectively.

However, if the degraded MB does not follow the uniform motion, to recover the degraded MV, the proposed approach applies the second proposed EC technique, named as the Improved Outer Boundary Matching Algorithm (IOBMA) in this paper. As illustrated in Fig. 5, similar to other boundary matching criterion-based EC techniques, in the proposed IOBMA, the MV of the degraded MB is selected among the candidate MVs according to a specific boundary matching criterion as follows:

$$n_{opt} = \arg\min_{n \in \{Candidate\ MVs\}} IOBMC^n \tag{5}$$

where

$$IOBMC^{n} = \left(IOBMC^{n}_{top} + IOBMC^{n}_{bottom} + IOBMC^{n}_{right} + IOBMC^{n}_{left}\right) \quad (6)$$

The $IOBMC^{n}_{top}$, $IOBMC^{n}_{bottom}$, $IOBMC^{n}_{right}$, $IOBMC^{n}_{left}$, and $IOBMC^{n}$ represent the boundary distortions on the top, bottom, right, left boundaries of the degraded MB and the total boundary distortion corresponding to the n^{th} candidate MV, respectively. The candidate MVs set includes the MVs of the MBs on the top, right, left, and bottom of the degraded MB, average and median MVs of the neighboring MBs and the zero MV.

As stated in Section 1, the error propagation issue due to the inaccurate estimation of the previous degraded MVs could affect the MV estimation of the remaining degraded MBs. Therefore, in addition to brightness information of the neighboring MBs, the proposed IOBMA tries to exploit the color information of the neighboring MBs to improve the accuracy of the MV estimation. Besides, to reduce the adverse effect of the error propagation on the MV estimation of the next degraded MVs, the boundary distortion corresponding to each candidate MV is calculated as the weighted average of the boundary distortions between the outer boundaries of the degraded MB and the corresponding ones in the candidate MB using (7)-(11).

$$IOBMC^{n}_{top} = w_{top} \times \frac{1}{\left|N_{top}\right|} \sum_{(x,y)\in N_{top}} \mathcal{D}(x, y-1)\Big|_{MV^{n}} \quad (7)$$

$$IOBMC^{n}_{left} = w_{left} \times \frac{1}{\left|N_{left}\right|} \sum_{(x,y)\in N_{left}} \mathcal{D}(x-1, y)\Big|_{MV^{n}} \quad (8)$$

$$IOBMC^{n}_{bottom} = w_{bottom} \times \frac{1}{\left|N_{bottom}\right|} \sum_{(x,y)\in N_{bottom}} \mathcal{D}(x, y+\mathcal{L}_{y})\Big|_{MV^{n}} \quad (9)$$

$$IOBMC^{n}_{right} = w_{right} \times \frac{1}{\left|N_{right}\right|} \sum_{(x,y)\in N_{right}} \mathcal{D}(x+\mathcal{L}_{x}, y)\Big|_{MV^{n}} \quad (10)$$

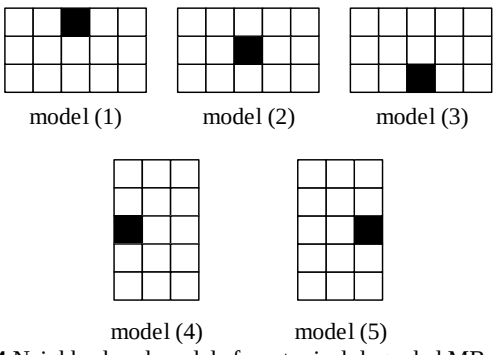

Fig. 4 Neighborhood models for a typical degraded MB. Each square represents an MB with a fixed size of 16 by 16 pixels [38]. The gray square in each model represents the position of the lost MB.

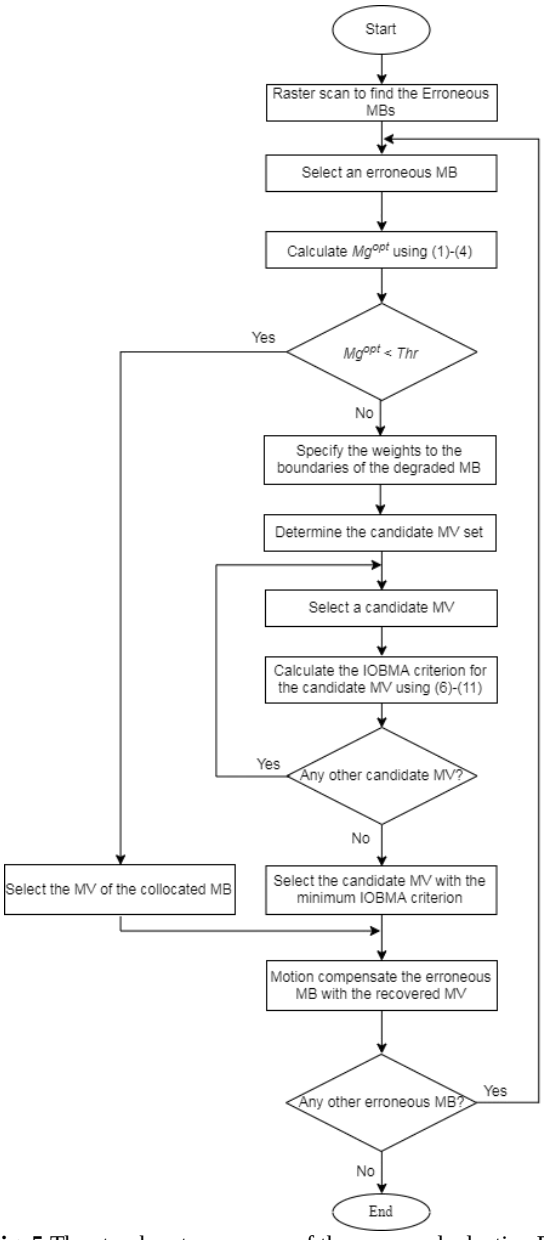

Fig. 5 The step-by-step process of the proposed adaptive EC approach.

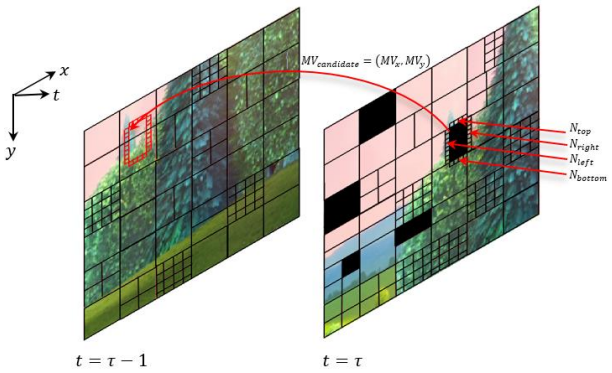

Fig. 6 Illustration of the candidate MB partition in the reference frame and the corresponding outer boundaries for two frames of a video sequence coded by H.264/AVC.

In (7)-(10), the MV^n represents the *n*-th candidate MV. N_{top}, N_{right}, N_{bottom}, and N_{left} contain the coordinates of the available pixels on the *top*, *right*, *bottom*, and *left* outer boundaries of the degraded MB. $|N_{poition}|$ denotes the cardinality of $N_{poition}$. w_{tpo}, w_{right}, w_{bottom}, and w_{left} stand for the weights specifically assigned to the *top*, *right*, *bottom*, and *left* outer boundaries of the degraded MB. $\mathcal{L}_x$ and $\mathcal{L}_y$ indicate the *x*- and *y*-dimension of the MB. $\mathcal{D}(p,q)\big|_{MV^n}$ represents the sum of absolute differences between the pixel located at position (*p*,*q*) in the current frame and the reference one in the reference frame according to the candidate motion vector, MV^n, as follows:

$$\begin{aligned}\mathcal{D}(p,q)\big|_{MV^n} &= \left|f_y(p,q,t)-f_y\left(p+MV_x^n,q+MV_y^n,t-1\right)\right| \\ &+\left|f_u(p,q,t)-f_u\left(p+MV_x^n,q+MV_y^n,t-1\right)\right| \\ &+\left|f_v(p,q,t)-f_v\left(p+MV_x^n,q+MV_y^n,t-1\right)\right| \quad (11)\end{aligned}$$

MV_x^n and MV_y^n represent the horizontal and vertical components of the *n*-th candidate MV, respectively. The $f_y(p,q,.)$, $f_u(p,q,.)$, and $f_v(p,q,.)$ represent the luminance and the chrominance components of the pixel located at the position (*p*,*q*) in the YUV color encoding system, respectively.

As illustrated in Fig. 6 the outer boundary pixels of an MB are taken from neighboring MBs. The neighboring MBs could be degraded, reconstructed, or intact. If the neighboring MB does not exist or it is degraded, the weight assigned to the corresponding boundary equals zero. However, to alleviate the error propagation issue, the available neighboring MBs, including the intact and previously reconstructed MBs, are weighted with different weights. In this regard, 1 and 0.5 are chosen as the weighting coefficients for the boundary distortions of the intact and the previously reconstructed MBs, respectively.

4 Simulation Results

4.1 Simulation Considerations

In this section, the performance of the proposed EC approach is compared with the state-of-the-art EC techniques including [37] and [38], DTBMA [23], and the well-known EC techniques BMA [17] and OBMA [18], Average MV (Mean) and Temporal Replacement (TR).

To evaluate the performance of the EC techniques, ten standard video sequences with different types of movement and textures are encoded in 4:2:0 format with H.264/AVC (JM 19.0) and the quantization parameter (QP) of 20. Since the Proposed EC approach is independent of the frame type and can be applied on both the P- and B-frames, for the sake of simulations simplicity, the picture structure is considered IPPP with GOP of 30 frames.

The performance is evaluated for 5%, 10%, and 20% random and slice errors. However, as the errors are applied randomly to the frames, to ensure that the location of the erroneous MBs within the frames does not impress the EC results, the experiments are repeated 15 times and the average PSNRs are selected as the final results.

4.2 Results Analysis

In this section, the objective and subjective quality assessments and also the corresponding computational complexity of the competing EC techniques are listed in Table 1-3. In order to evaluate the performances and the computational complexities of the competing EC techniques, the average PSNR (Peak Signal to Noise Ratio) and the reconstruction time per MB (in msec) are used as the metrics, respectively.

Tables 1 and 2 represent the performances of the competing EC techniques for different video sequences in the presence of random and slice errors, respectively. A general look at Table 1 yields that, depending on the video sequence, the proposed EC approach can achieve up to 5.78, 2.99, 2.81, 1.62, 1.30, 1.23, 0.61 and 0.45 dB higher PSNRs than the TR, Mean, [37], DBMA, BMA, DTBMA, [38] and the OBMA techniques, respectively. Also, regarding the Table 2 and 3, it can be observed that under the 20% BLR slice error, while maintaining the computational complexity of the proposed EC approach at an acceptable level, the improvements over the reference EC techniques could rise up to 2.92, 2, 1.75, 0.62 and 2.01 dB compared with the DBMA, BMA, DTBMA, Ref. [38] and the OBMA techniques, respectively.

Another point regarding Tables 1 and 2 are related to the effect of the video content on the performances of the different EC techniques. To the best of our knowledge, there is no EC technique outperforming the whole EC techniques in the video sequences of various contents. This could also be verified by comparing the performances of the reference EC techniques in Tables 1 and 2. In Table 2, for example, [38] outperforms the other reference EC techniques in the video sequences such as the "Bus" and "Crew" under the 20% BLR, whereas in the "Football" and "Ice" sequences, the highest performances belong to the DTBMA and [37], respectively. This is also the case for the other EC techniques. For example, in the "Soccer" sequence in Table 1, the simple EC technique, Mean, outperforms the state-of-the-art EC technique, [37], and/or in the "Hall" sequence, the TR provides the highest PSNR, compared with the competing EC techniques. The video content, from the MVs variations in the consecutive frames viewpoint, is responsible for this event. For example, in the "Hall" video sequence, in which the camera motion is static and the object own regular structure and slow uniform motion, the MVs of the MBs within the frames are mostly zero with no significant residual information. Hence, the TR is expected to

Table 1 Objective quality assessments for random error.

Resolution	Sequence	Video content (camera motion) / (object motion/structure)	Block Loss Rate [%]	Average PSNR [dB] for random error									
				Erroneous frame	OBMA	DTBMA	DBMA	Ref. [37]	BMA	Mean	TR	Ref. [38]	Proposed Approach
CIF	Bus	Fast [pan] / Fast [uniform] / regular	5	20.27	49.39	48.65	48.49	47.09	48.60	46.88	43.74	49.38	49.52
			10	17.24	45.49	44.65	44.34	43.11	44.60	42.71	40.18	45.49	45.62
			20	14.37	41.28	40.57	40.11	39.35	40.41	38.80	36.75	41.56	41.65
	Football	Fast [pan] / Fast [complex] / irregular	5	19.79	39.55	39.65	39.56	37.67	39.61	38.74	37.79	39.53	39.92
			10	16.78	36.07	36.19	36.05	34.23	36.16	35.33	34.44	36.04	36.40
			20	13.92	32.55	32.79	32.62	30.92	32.76	31.92	31.18	32.52	32.89
	Foreman	Slow [pan] / Fast [complex] / regular	5	18.53	55.25	54.78	54.75	53.94	54.50	53.71	52.51	55.21	55.60
			10	15.50	51.21	50.75	50.54	49.84	50.42	49.30	48.50	51.09	51.61
			20	12.64	46.84	46.61	46.28	45.38	46.28	45.12	44.50	46.67	47.29
	Coastguard	Slow [pan] / Slow [uniform] / regular	5	19.29	60.08	59.24	59.35	59.65	59.29	58.85	56.08	60.09	60.24
			10	16.26	55.88	55.00	55.14	55.22	55.09	54.43	52.17	55.94	56.14
			20	13.42	51.17	50.41	50.40	50.46	50.40	49.57	47.66	51.43	51.54
	Hall	Static / Slow [uniform] / regular	5	19.13	52.49	51.99	51.96	52.40	51.97	51.26	52.34	52.54	52.50
			10	16.08	48.90	48.48	48.44	48.75	48.43	47.65	48.71	48.92	48.90
			20	13.24	45.27	44.83	44.71	45.19	44.76	43.97	45.13	45.37	45.33
	Stefan	Slow [pan] / Fast [complex] / irregular	5	19.22	46.42	46.03	46.02	43.84	46.04	45.65	42.74	46.36	46.56
			10	16.20	42.57	42.27	42.18	40.07	42.27	41.96	39.07	42.50	42.73
			20	13.34	38.77	38.59	38.37	36.18	38.57	38.19	35.61	38.73	38.99
	Average		5	19.37	50.53	50.06	50.02	49.10	50.00	49.18	47.53	50.52	50.72
			10	16.35	46.69	46.22	46.11	45.20	46.16	45.23	43.85	46.66	46.90
			20	13.49	42.65	42.30	42.08	41.25	42.20	41.26	40.14	42.71	42.94
4CIF	City	Slow [pan] / Static	5	19.29	53.92	53.43	53.36	53.43	53.04	52.37	50.99	53.78	54.00
			10	16.39	50.51	50.03	49.92	49.94	49.58	48.99	47.57	50.29	50.60
			20	13.60	46.57	46.16	45.96	45.89	45.75	45.22	43.79	46.31	46.65
	Ice	Static / Slow [uniform] / regular	5	18.87	56.30	55.42	55.28	55.65	55.35	53.73	52.78	56.34	56.65
			10	15.96	52.16	51.39	51.13	51.48	51.29	49.59	48.90	52.21	52.58
			20	13.15	47.74	47.09	46.57	47.01	46.97	45.50	44.86	47.76	48.19
	Crew	Static [pan] / Slow [complex] / irregular	5	19.70	51.10	50.78	50.67	50.32	50.76	50.10	50.00	51.07	51.40
			10	16.80	47.55	47.34	47.16	46.86	47.27	46.59	46.51	47.53	47.86
			20	14.00	43.90	43.84	43.53	43.10	43.67	43.09	42.86	43.88	44.24
	Soccer	Slow [pan] / Slow [complex] / irregular	5	19.18	52.67	52.42	52.27	51.13	52.11	51.57	47.86	52.48	52.87
			10	16.27	49.10	48.94	48.73	47.52	48.55	48.11	44.38	48.84	49.35
			20	13.48	45.03	45.05	44.68	43.24	44.52	44.18	40.56	44.69	45.28
	Average		5	19.26	53.50	53.01	52.89	52.63	52.81	51.94	50.41	53.42	53.73
			10	16.35	49.83	49.43	49.23	48.95	49.17	48.32	46.84	49.72	50.10
			20	13.56	45.81	45.53	45.19	44.81	45.23	44.50	43.02	45.66	46.09

provide good results. However, in the video sequences with more complex movements and irregular structures, such as the "Football", in which the MVs scattering is high, its performance is exposed to severe degradation.

A closer look at Tables 1 and 2 indicates that, in addition to the video content, the type of error can also affect the performances of the EC techniques. Regarding the average performances for the 4CIF resolution sequences, for instance, the Ref. [37] outperforms most of the reference EC techniques under the 20% slice error, whereas its performance is severely degraded in the presence of the random error, compared with other reference EC techniques. This holds true for the whole EC techniques so that, in terms of the average PSNR, the reference EC techniques do not follow an identical order in the different video sequences.

However, regarding the Tables 1 and 2, denotes that, in the presence of both the random and slice errors, the proposed EC approach, not only outperforms the reference EC techniques in most of the test sequences, but also provides the best performance on average, compared with the reference EC techniques.

Note that the performances listed in Tables 1 and 2 represent the PSNRs per frame, averaged over the whole frames within the GoP. This means that, for the Proposed EC approach, in some frames, the amount of the performance improvement over the reference EC techniques might be much higher than this, and of course in some frames, not. Therefore, to further verify the performances of the EC techniques, frame-by-frame PSNR evaluations of the competing EC techniques are also presented in Fig. 7-10.

Table 2 Objective quality assessments for slice error.

Resolution	Sequence	Video content (camera motion) / (object motion/structure)	Block Loss Rate [%]	Average PSNR (dB) for slice error									
				Erroneous frame	OBMA	DTBMA	DBMA	Ref. [37]	BMA	Mean	TR	Ref. [38]	Proposed Approach
CIF	Bus	Fast [pan] / Fast [uniform] / regular	5	20.36	48.80	48.88	47.35	48.88	48.59	47.17	44.47	49.77	49.81
			10	17.14	44.13	44.26	42.76	44.19	43.92	42.64	40.43	45.26	45.34
			20	13.94	38.72	39.52	37.79	39.61	38.86	37.61	36.49	40.53	40.71
	Football	Fast [pan] / Fast [complex] / irregular	5	19.67	40.16	40.44	40.13	39.49	40.26	39.86	39.24	40.16	40.58
			10	16.57	35.97	36.41	36.08	35.58	36.22	35.72	35.16	35.99	36.51
			20	13.50	31.40	31.87	31.54	31.13	31.68	31.35	30.75	31.42	31.98
	Foreman	Slow [pan] / Fast [complex] / regular	5	18.49	54.68	54.30	53.41	54.07	53.89	53.69	52.37	54.84	55.40
			10	15.30	50.12	49.86	49.01	50.03	49.59	49.12	48.33	50.62	51.24
			20	12.22	45.17	45.21	44.04	45.03	44.73	43.97	43.85	45.66	46.23
	Coastguard	Slow [pan] / Slow [uniform] / regular	5	19.53	44.31	44.24	44.14	44.35	44.25	44.30	43.69	44.41	44.43
			10	16.16	56.10	55.57	55.05	56.30	55.67	55.58	52.79	56.73	57.03
			20	13.06	49.69	49.95	49.36	50.74	49.70	49.46	47.62	51.14	51.70
	Hall	Static / Slow [uniform] / regular	5	19.17	52.32	51.96	51.79	52.60	51.75	51.77	52.47	52.63	52.46
			10	15.95	48.60	48.01	47.69	48.83	47.87	47.28	48.72	48.86	48.77
			20	12.82	44.09	43.57	43.32	44.57	43.22	42.31	44.49	44.60	44.50
	Stefan	Slow [pan] / Fast [complex] / irregular	5	19.17	48.66	47.97	47.40	47.79	47.70	47.94	45.59	48.66	48.91
			10	16.02	43.17	42.58	41.91	42.11	42.37	42.78	40.02	43.26	43.50
			20	12.91	38.16	37.79	37.14	36.97	37.49	37.78	35.37	38.42	38.59
	Average		5	19.40	48.16	47.96	47.37	47.86	47.74	47.45	46.31	48.41	48.60
			10	16.19	46.35	46.11	45.42	46.17	45.94	45.52	44.24	46.79	47.07
			20	13.07	41.21	41.32	40.53	41.34	40.95	40.41	39.76	41.96	42.28
4CIF	City	Slow [pan] / Static	5	19.19	53.36	52.05	51.93	53.27	51.97	52.15	50.66	53.36	53.51
			10	16.18	49.99	48.92	48.82	50.05	48.85	48.93	47.53	50.03	50.20
			20	13.17	45.36	44.43	44.21	45.17	44.36	44.14	43.12	45.31	45.60
	Ice	Static / Slow [uniform] / regular	5	18.76	56.15	55.38	54.49	56.34	55.65	54.52	53.42	56.48	56.24
			10	15.72	51.50	50.76	49.97	51.91	51.07	49.85	49.21	51.94	51.73
			20	12.74	46.22	45.64	44.74	46.87	45.70	44.39	44.39	46.79	46.85
	Crew	Static [pan] / Slow [complex] / irregular	5	19.67	50.77	50.62	49.87	50.60	50.52	50.56	50.16	50.87	51.16
			10	16.59	47.02	46.90	46.21	46.92	46.86	46.59	46.48	47.16	47.37
			20	13.56	42.83	42.90	42.08	42.87	42.68	42.44	42.43	43.02	43.24
	Soccer	Slow [pan] / Slow [complex] / irregular	5	19.10	52.00	51.74	51.17	51.98	51.83	51.75	48.63	52.04	52.18
			10	16.09	47.85	47.85	47.00	48.01	47.80	47.76	44.66	47.96	48.30
			20	13.04	43.01	43.12	42.20	43.11	42.95	42.90	39.92	43.08	43.54
	Average		5	19.18	53.07	52.45	51.87	53.05	52.49	52.24	50.72	53.19	53.27
			10	16.14	49.09	48.61	48.00	49.22	48.64	48.28	46.97	49.27	49.40
			20	13.13	44.35	44.02	43.31	44.50	43.92	43.47	42.46	44.55	44.81

Regarding Fig. 7 and the corresponding PSNRs listed in Table 2, for example, it can be observed that, in the "Coastguard" sequence, the proposed EC approach provides at least 0.55 dB higher performance than the reference EC technique with the highest average PSNR (i.e., [38]). However, as seen in Fig. 7, this amount of improvement over [38] increases to more than 4.3 dB in some frames. Therefore, the quality of the reconstructed video sequence is expected to increase considerably in those frames.

This is also the case for the reference EC techniques. Regarding the performances of the reference EC techniques for the "Foreman" sequence in Table 1, for example, [38] outperforms the DTBMA by more than 0.34 dB. However, Fig. 9 yields that in the 12th frame the achievable PSNR for the DTBMA is 2.8 dB higher than the [38]. Similarly, as seen in Fig. 10, the PSNR for the OBMA in the 22nd frame is 1.2 lower than the performance of the DTBMA, while the performances of the OBMA and DTBMA techniques listed in Table 1 denote that, for the "Ice" sequence, the OBMA outperforms the DTBMA by 0.65 dB.

As stated before, a typical EC technique does not necessarily provide the best reconstruction results for the video sequences of different contents, compared with other EC techniques. Regarding Fig. 7-10, it can be observed that this point also holds true for different frames of a video sequence, so that the reference EC techniques do not follow an identical order in the consecutive frames. For instance, as seen in Fig. 9, [37] outperforms the DTBMA by more than 1.16 dB in the 9th frame, while, in the 12th frame, its performance decreases to 3.44 dB below the performance of the DTBMA. Many factors could be responsible for this event, such as the content of the degraded frame in the erroneous regions from the motion type and structure

Table 3 average reconstruction time per MB under 20% BLR slice error.

Resolution	Sequence	Reconstruction time (msec) per MB under 20% BLR slice error								
		OBMA	DTBMA	DBMA	Ref. [37]	BMA	Mean	TR	Ref. [38]	Proposed Approach
CIF	Bus	5	12	3	4	5	1	1	3	5
	Football	5	12	3	9	5	1	1	5	5
	Foreman	5	12	3	1	5	1	1	4	5
	Coastguard	5	12	3	1	5	1	1	2	5
	Hall	5	12	3	1	5	1	1	2	5
	Stefan	5	12	3	3	5	1	1	3	5
	Average	5.00	12.00	3.00	3.17	5.00	1.00	1.00	3.17	5.00
4CIF	City	8	16	6	4	4	4	3	6	9
	Ice	8	16	6	4	4	4	3	6	9
	Crew	8	16	6	4	4	4	3	8	9
	Soccer	8	16	6	4	4	4	3	6	9
	Average	8.00	16.00	6.00	4.00	4.00	4.00	3.00	6.50	9.00

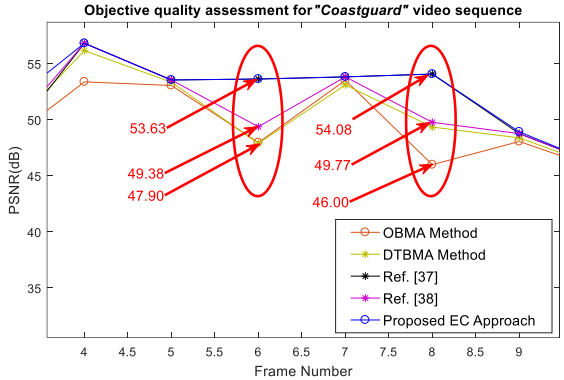

Fig. 7 Frame-by-frame PSNR evaluation for the CIF resolution "Coastguard" sequence under 20% slice error.

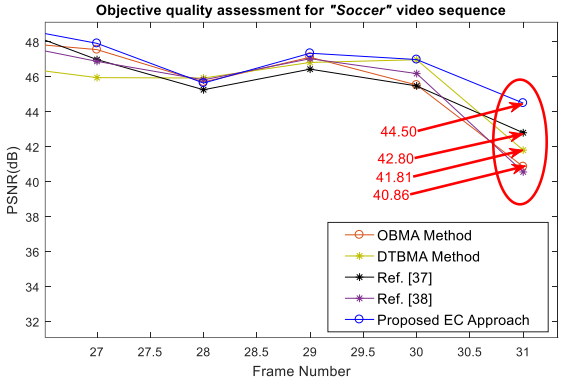

Fig. 8 Frame-by-frame PSNR evaluation for the 4CIF resolution "Soccer" sequence under 20% slice error.

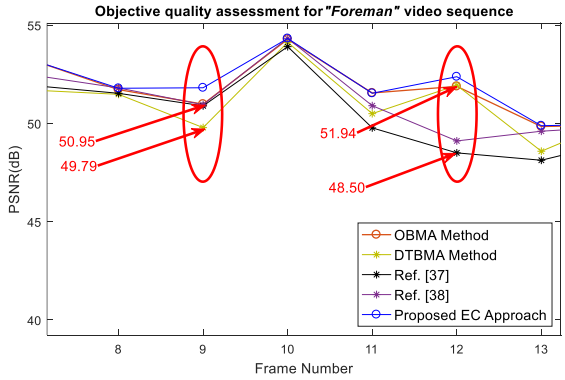

Fig. 9 Frame-by-frame PSNR evaluation for the CIF resolution "Foreman" sequence under 10% random error.

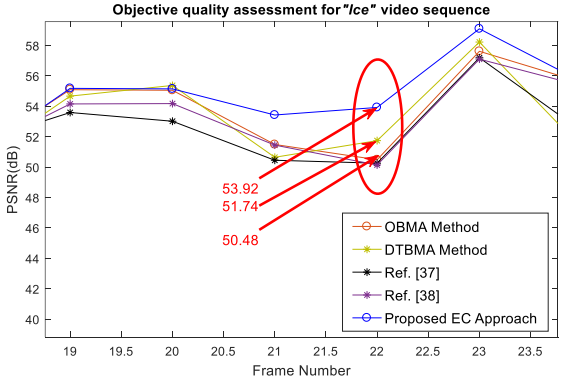

Fig. 10 Frame-by-frame PSNR evaluation for the 4CIF resolution "Ice" sequence under 10% random error.

type viewpoint, the random position of the lost MBs in the frame, the error propagation issue, etc. Regarding the motion type, for instance, due to the random position of the degraded MBs within the frame, the reliability and the amount of the information exploited for MV recovery may vary depending on the motion changes around the degraded MB due to both the camera and object motions. In the "Foreman" sequence, in which the camera motion is slow and the object motion is fast and uniform, the temporal MV scattering in the consecutive frames could play an important role on the performance of the MV recovery. In the 9th frame, for example, the temporal MV scattering is low, and hence, [37] is expected to provide appropriate reconstruction results. In the 12th frame, however, where the temporal MV scattering tends to increase due to the sudden change of the object movement in the foreground, its performance goes under severe degradation.

To visually display the performance of the proposed EC approach, three instances of the subjective quality assessments of the competing EC techniques are also presented in Fig. 11 in the presence of both random and slice errors. As seen, due to more accurate estimates of

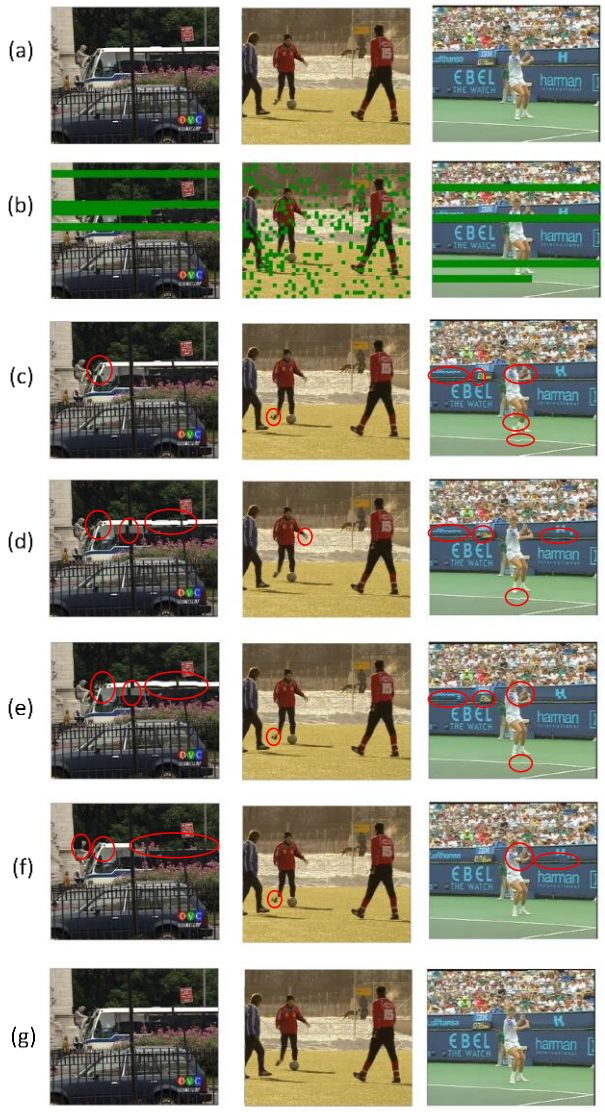

Fig. 11 Subjective quality assessments in the presence of 20% slice and random errors. a) Intact frame, b) degraded frame, c) EC with OBMA, d) EC with DTBMA, e) EC with [38], f) EC with [37], and g) EC with the proposed approach.

the lost MVs, the proposed EC approach provides better reconstruction quality than the reference EC techniques, from the output blocky artifacts viewpoint.

5 Conclusion

In this paper, a novel EC approach was presented to estimate the MVs of the degraded MBs through analyzing the video scene from the motion type and the spatial information reliability point of view. To this end, the proposed EC approach first analyzes the motion type of the available MBs adjacent to the degraded MB to estimate whether the degraded MB had a uniform or complex motion.

For the uniform motion MBs, the most appropriate MV for motion compensation is the MV of the collocated MB. For the complex motion MBs, however, due to the high MVs scattering, the degraded MV needs to be estimated regarding other information within the video scene. In this regard, the boundary matching criterion-based EC techniques usually yield higher performances compared with other TEC techniques. However, the performance of these techniques is highly dependent on the correct spatial information on the boundaries of the degraded MB, so that their performances are exposed to severe degradation in the presence of the slice error with high Block Loss Rates (BLRs). Therefore, in this paper, a new EC technique is proposed which tries to improve the performance of the boundary matching algorithms by exploiting both the color information and the unreliability of the boundary pixels.

The experimental results for the various video sequences and BLRs indicate that with no considerable increase in the computational complexity, the proposed EC approach can enhance the average PSNR performance of the EC up to 1.5, 0.82, 1.28, 0.43, and 0.45 dB, compared with the state-of-the-art EC techniques, DBMA, DTBMA, [37], [38], and OBMA, respectively.

References

[1] S. Lin and D. J. Costello, *Error control coding: fundamentals and applications*. Prentice-Hall, 1983.

[2] J. W. Wells and A. Chatterjee, "Error-resilient video encoding using parallel independent signature processing," *IEEE Transactions on Circuits and Systems for Video Technology*, Vol. 27, No. 5, pp. 1077–1090, 2017.

[3] H. S. Gang, S. I. Chowdhury, C. S. Park, G. R. Kwon, and J. Y. Pyun, "Error resilient multiple reference selection for wireless video transmission," *IEICE Transactions on Communications*, Vol. E100.B, No. 4, pp. 657–665, 2017.

[4] H. Ha and C. Yim, "Unequal luby transform based on block weight shift (ULT-BWS) for error resilient video transmission," *Wireless Personal Communications*, Vol. 89, No. 4, pp. 1103–1121, 2016.

[5] N. Gadgil and E. J. Delp, "VPx error resilient video coding using duplicated prediction information," *Electronic Imaging*, Vol. 2016, No. 2, pp. 1–6, 2016.

[6] L. Zhang, Q. Peng, X. Wu, and Q. Wang, "SSIM-based error resilient video coding over packet-switched networks," *Journal of Signal Processing Systems*, Vol. 74, No. 1, pp. 103–113, 2014.

[7] M. Kazemi, S. Shirmohammadi, and K. H. Sadeghi, "A review of multiple description coding techniques for error-resilient video delivery," *Multimedia Systems*, Vol. 20, No. 3, pp. 283–309, 2014.

[8] H. G. Yakhdan, M. Khademi, and J. Chitizadeh, "A new unequal error protection technique based on the mutual information of the MPEG-4 video frames over wireless networks," *Iranian Journal of Electrical and Electronic Engineering*, Vol. 5, No. 1, pp. 23–31, 2009.

[9] J. Liu, G. Zhai, X. Yang, B. Yang, and L. Chen, "Spatial error concealment with an adaptive linear predictor," *IEEE Transactions on Circuits and Systems for Video Technology*, Vol. 25, No. 3, pp. 353–366, 2015.

[10] Y. H. Lee, C. H. Lin, C. C. Chen, S. Y. Lin, and B. S. Huang, "The video spatial error concealment algorithm using separately-directional interpolation technique," *Journal of Signal Processing Systems*, Vol. 88, No. 1, pp. 13–27, 2017.

[11] H. Ni and Y. Li, "Spatial error concealment algorithm based on adaptive edge threshold and directional weight," *International Journal of Pattern Recognition and Artificial Intelligence*, Vol. 31, No. 08, 2017.

[12] A. Akbari, M. Trocan, and B. Granado, "Joint-domain dictionary learning-based error concealment using common space mapping," in *22nd International Conference on Digital Signal Processing (DSP)*, pp. 1–5, 2017.

[13] M. Mohammadzadeh Qaratlu and M. Ghanbari, "Intra-frame loss concealment based on directional extrapolation," *Signal Processing: Image Communication*, Vol. 26, No. 6, pp. 304–309, 2011.

[14] B. Chung and C. Yim, "Hybrid error concealment method combining exemplar-based image inpainting and spatial interpolation," S*ignal Processing: Image Communication*, Vol. 29, No. 10, pp. 1121–1137, 2014.

[15] P. K. Rajani and A. Khaparde, "Comparison of frequency selective extrapolation and patch matching algorithm for error concealment in spatial domain," in *Proceedings of the 8th International Conference on Signal Processing Systems (ICSPS 2016)*, Auckland, New Zealand, pp. 70–74, 2016.

[16] A. Akbari, M. Trocan, and B. Granado, "Sparse recovery-based error concealment," *IEEE Transactions on Multimedia*, Vol. 19, No. 6, pp. 1339–1350, 2017.

[17] W. M. Lam, A. R. Reibman, and B. Liu, "Recovery of lost or erroneously received motion vectors," in *IEEE International Conference on Acoustics, Speech, and Signal Processing*, Vol. 5, pp. 417–420 Vol.5, 1993.

[18] T. Thaipanich, P. H. Wu, and C. C. J. Kuo, "Video error concealment with outer and inner boundary matching algorithms," *Applications of Digital Image Processing XXX*, Vol. 6696, p. 669607, 2007.

[19] C. Yu, C. Cheng, H. Jin, and J. Zhou, "Efficient multiple-reference temporal error concealment algorithm based on H.264/AVC," in *International Conference on Human Centered Computing*, Springer, Cham, pp. 497–509, 2016.

[20] T. L. Lin, N. C. Yang, R. H. Syu, C. C. Liao, and W. L. Tsai, "Error concealment algorithm for HEVC coded video using block partition decisions," in *IEEE International Conference on Signal Processing, Communication and Computing (ICSPCC)*, pp. 1–5, 2013.

[21] T. L. Lin, W. C. Chen, and C. K. Lai, "Recovery of lost motion vectors using encoded residual signals," *IEEE Transactions on Broadcasting*, Vol. 59, pp. 705–716, 2013.

[22] X. Chen, Y. Y. Chung, and C. Bae, "Dynamic multi-mode switching error concealment algorithm for H.264/AVC video applications," *IEEE Transactions on Consumer Electronics*, Vol. 54, No. 1, pp. 154–162, 2008.

[23] S. M. Marvasti-Zadeh and H. Ghanei-Yakhdan, "Video temporal error concealment using improved directional boundary matching algorithm," *Turkish Journal of Electrical Engineering & Computer Sciences*, Vol. 24, No. 6, pp. 5195–5209, 2016.

[24] S. M. Marvasti Zadeh, H. Ghanei Yakhdan, and S. Kasaei, "An efficient adaptive boundary matching algorithm for video error concealment," *Iranian Journal of Electrical and Electronic Engineering*, Vol. 10, No. 3, pp. 188–202, 2014.

[25] W. N. Lie, C. M. Lee, C. H. Yeh, and Z. W. Gao, "Motion vector recovery for video error concealment by using iterative dynamic-programming optimization," *IEEE Transactions on Multimedia*, Vol. 16, No. 1, pp. 216–227, 2014.

[26] X. Wei, H. W. Tseng, J. W. Jhang, T. H. Su, Y. C. Yu, Y. Wen, Z. Liu, T. L. Lin, S. L. Chen, Y. S. Chiou, and H. Y. Lee, "Video error concealment method using motion vector estimation propagation," in *International Conference on Applied System Innovation (ICASI)*, pp. 1335–1338, 2017.

[27] S. Cui, H. Cui, and K. Tang, "An effective error concealment scheme for heavily corrupted H.264/AVC videos based on Kalman filtering," *Signal, Image and Video Processing*, Vol. 8, No. 8, pp. 1533–1542, 2014.

[28] A. Radmehr and A. Ghasemi, "Error concealment via particle filter by Gaussian mixture modeling of motion vectors for H.264/AVC," *Signal, Image and Video Processing*, Vol. 10, No. 2, pp. 311–318, 2016.

[29] S. Cui, H. Cui, and K. Tang, "Error concealment via Kalman filter for heavily corrupted videos in H.264/AVC," *Signal Processing: Image Communication*, Vol. 28, No. 5, pp. 430–440, 2013.

[30] H. Ghanei-Yakhdan, "A novel dynamic temporal error concealment technique for video sequences using a competitive neural network," in the *1st Iranian Conference on Pattern Recognition and Image Analysis*, 2013.

[31] Y. Chen, Y. Hu, O. C. Au, H. Li, and C. W. Chen, "Video error concealment using spatio-temporal boundary matching and partial differential equation," *IEEE Transactions on Multimedia*, Vol. 10, No. 1, pp. 2–15, 2008.

[32] M. Ko, J. Hong, and J. Suh, "Error detection scheme for the H.264/AVC using the RD optimized motion vector constraints," *IEEE Transactions on Consumer Electronics*, Vol. 58, No. 3, pp. 955–962, 2012.

[33] X. Qian, G. Liu, and H. Wang, "Recovering connected error region based on adaptive error concealment order determination," *IEEE Transactions on Multimedia*, Vol. 11, No. 4, pp. 683–695, 2009.

[34] Y. Bo and N. Kam Wing, "Analysis and detection of MPEG-4 visual transmission errors over error-prone channels," *IEEE Transactions on Consumer Electronics*, Vol. 49, No. 4, pp. 1424–1430, 2003.

[35] W. Yao and Z. Qin-Fan, "Error control and concealment for video communication: a review," *Proceedings of the IEEE*, Vol. 86, No. 5, pp. 974–997, 1998.

[36] K. C. Pathak, S. Singh, and J. N. Patel, "Error detection and concealment algorithm for compressed video transmission," in *IEEE Region 10 Humanitarian Technology Conference (R10-HTC)*, pp. 1–5, Dec. 2016.

[37] D. H. Kim, Y. J. Kwon, and K. H. Choi, "Motion-vector refinement for video error concealment using downhill simplex approach," *ETRI Journal*, Vol. 40, No. 2, pp. 266–274, 2018.

[38] S. M. Zabihi, H. Ghanei-Yakhdan, and N. Mehrshad, "Adaptive temporal error concealment method based on the MB behavior estimation in the video," in *7th International Conference on Computer and Knowledge Engineering (ICCKE)*, pp. 193–198, 2017.

S. M. Zabihi received the B.Sc. and M.Sc. degrees in Telecommunication Engineering from the Department of Telecommunication, Faculty of Electrical and Computer Engineering, Birjand University, Birjand, Iran, in 2009 and 2012, respectively. He is currently a Ph.D. candidate in the Department of Electrical Engineering at Yazd University, Yazd, Iran. His research interests include digital image and video processing, video error concealment, and cooperative wireless communication.

H. Ghanei-Yakhdan received the B.Sc. degree in Electrical Engineering from Isfahan University of Technology, Isfahan, Iran, in 1989, the M.Sc. degree in 1993 from K. N. Toosi University of Technology, Tehran, Iran, and the Ph.D. degree in 2009 from Ferdowsi University of Mashhad, Mashhad, Iran. Since 2009, he has been an Assistant Professor with the Department of Electrical Engineering, Yazd University. His research interests are in digital video and image processing, error concealment and error-resilient video coding, and object tracking.

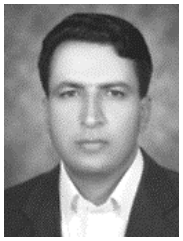

N. Mehrshad received the B.Sc. degree from Ferdowsi University of Mashhad, Mashhad, Iran, in 1995 and the M.Sc. and Ph.D. degrees from Tarbiat Modares University, Tehran, Iran, in 1998 and 2005, respectively, both in Biomedical Engineering. He is currently an Associate Professor in the Department of Electrical and Computer Engineering, University of Birjand, Birjand, Iran. His research interests include computer vision, digital signal and image processing, biometrics, and biomedical data mining.